

UNIVERSITY OF TARTU
Faculty of Science and Technology
Institute of Physics

Eero Vaher

VALIDATION OF SMART STELLAR ATMOSPHERE MODELS

Bachelor's thesis (12 ECTS)

Supervisors:
Anna Aret
Boris Deshev

Tartu 2015

Contents

Introduction	4
1 Background	5
1.1 Models of stellar atmospheres	5
1.1.1 The radiative transfer equation	5
1.1.2 Flux constancy	6
1.1.3 Geometry	7
1.1.4 Hydrostatic equilibrium	8
1.1.5 Local thermodynamic equilibrium	8
1.1.6 Additional factors	10
1.2 The formation of stellar spectra	10
1.2.1 Continuous absorption	11
1.2.2 Line absorption	12
1.3 Atmospheric parameters	12
2 Observational data	14
2.1 Selection criteria	14
2.2 Stellar sample	14
2.3 Observed spectra	15
2.4 Data processing	15
2.4.1 Radial velocities	15
2.4.2 Normalization	16
2.4.3 Equivalent widths	16
3 Computations and analysis	17
3.1 Program SMART	17
3.2 Model computations	18
3.3 Surface gravity	19
3.4 Effective temperature	20

3.5 Spectral broadening	22
4 Results and discussion	23
Summary	25
Kokkuvõte	26
Acknowledgements	27
Bibliography	28
A Comparison of synthetic and observed spectra	30
Lihtlitsents	37

Introduction

Stellar spectra provide most of the information that is known about the stars, such as their chemical composition, rotation, magnetic fields etc. The light that makes up the spectrum of a star is radiated by its outer layers that are called a stellar atmosphere. Understanding stellar atmospheres is therefore very important in all of stellar astrophysics. Because spectra are influenced by very many physical variables it is not usually possible to deduce directly from the spectra the exact values of the parameters of stellar atmospheres and comparisons with synthetic spectra computed from atmospheric models must be used. At present it is not possible to create a stellar atmosphere model that could be used to study all types of stars, so there are different models for different types of stars.

SMART (Stellar Model Atmospheres and Radiative Transfer) is a computer program written in the Tartu Observatory for computing atmospheric models and synthetic spectra of moderately hot stars. SMART is capable of taking into account light-induced drift, which might help explain the properties of chemically peculiar stars (see Sagar et al. (2009)).

SMART has not yet been used for determining the parameters of stellar atmospheres. The purpose of this work is to find out what is the temperature range of the stars that can be accurately modelled with SMART and how exactly can SMART be used for stellar temperature and surface gravity estimation. This also includes writing software to implement the suitable parameter estimation methods.

This thesis is divided into four parts. Chapter 1 gives a short overview of stellar atmospheres and their modelling. Chapter 2 describes the observed stellar spectra used in this work and the processing of observational data. The description of computer modelling and stellar parameter estimation is provided in Chapter 3 and the results and implications are discussed in Chapter 4.

Chapter 1

Background

1.1 Models of stellar atmospheres

A model of a stellar atmosphere is the set of physical properties of the stellar plasma as a function of depth, though often optical depth (see Equation 1.4) is used instead of geometrical depth (Gray, 2005, p. 170). An atmospheric model of a star can be tested by comparing the synthetic spectrum calculated from the model with an observed stellar spectrum.

1.1.1 The radiative transfer equation

The specific intensity of radiation is defined as

$$I_\nu = \frac{d^4 E_\nu}{\cos \theta dA d\omega dt d\nu} \quad (1.1)$$

where E_ν is the energy of radiation in the frequency range $(\nu, \nu + d\nu)$ emitted from a surface dA at an angle θ from its surface normal into the solid angle $d\omega$ during the time dt . If radiation with specific intensity I_ν travels through a layer of matter with the mass absorption coefficient κ_ν (with units cm^2/g), density ρ and thickness dx , then the change of specific intensity will be

$$dI_\nu = -\kappa_\nu \rho I_\nu dx. \quad (1.2)$$

If the matter is also emitting radiation, then the change in intensity will be

$$dI_\nu = -\kappa_\nu \rho I_\nu dx + j_\nu \rho dx \quad (1.3)$$

where j_ν is the emission coefficient. If we define the optical depth corresponding to the geometrical length L as

$$\tau_\nu = \int_0^L \kappa_\nu \rho dx \quad (1.4)$$

and the source function as

$$S_\nu = \frac{j_\nu}{\kappa_\nu}, \quad (1.5)$$

then we can write the equation 1.3 as

$$\frac{dI_\nu}{d\tau_\nu} = -I_\nu + S_\nu \quad (1.6)$$

and its solution in line-of-sight coordinates (see (Gray, 2005, p. 127-129) for details) as

$$I_\nu(\tau_\nu) = I_\nu(0)e^{-\tau_\nu} + \int_0^{\tau_\nu} S_\nu(t_\nu)e^{-(\tau_\nu-t_\nu)} dt_\nu. \quad (1.7)$$

The interpretation of Equation 1.7 is quite straightforward. Radiation is being emitted at the optical depths where $S_\nu > 0$, but the specific intensity of the emitted radiation and also the original radiation present at $\tau_\nu = 0$ decays exponentially as it propagates through the medium.

If the value of the source function would be known for all frequencies and optical depths, then it would be possible to use the Equation 1.7 to compute the specific intensities at all frequencies. The source function can be computed from the parameters of matter, but those parameters are also influenced by radiation and therefore by the source function. This is the reason why models of stellar atmospheres that are based on solving the radiative transfer equation are iterative, making improvements to some initial model until convergence is achieved.

1.1.2 Flux constancy

The flux of radiation is defined as

$$F_\nu = \frac{d^3 E_\nu}{dA dt dv} \quad (1.8)$$

and can also be written as

$$F_\nu = \oint I_\nu \cos \theta d\omega. \quad (1.9)$$

Flux describes the total net energy flow through a surface while specific intensity contains more detailed information about the directional distribution of radiation. Specific intensity is independent of the distance of the source and can only be directly measured if the surface of the source can be resolved. The dependence of flux on the distance of the source is an inverse square law. Only flux can be directly measured if the surface of the source cannot be resolved.

The energy radiated by stars originates from the thermonuclear reactions that take place in their cores. Energy is not released nor is it absorbed in the outer layers, it merely propagates through them. The main mechanisms of energy transportation are radiative transport and, in the case of cooler stars, convection (Gray, 2005, p. 141). The total energy flux in a stellar atmosphere cannot change, only its spectral distribution can (Gray, 2005, p. 136).

The flux of radiation inside the stellar atmospheres can be estimated by using Equations 1.7 and 1.9. The source function in Equation 1.7 can be computed based on the temperature, chemical composition and other parameters of matter, but those parameters are influenced by radiation. This means that a model of a stellar atmosphere is not automatically internally consistent. If the value of flux is not constant for all depths, the temperature distribution must be corrected and the computations reiterated until flux constancy is achieved within sufficient accuracy. (Gray, 2005, p. 185)

1.1.3 Geometry

In the case of stellar atmospheres distances are usually measured from the stellar surface, not from the centre of the star, and also along the line of sight. Optical depth $\tau_\nu \approx 0$ therefore corresponds to the surface of the star.

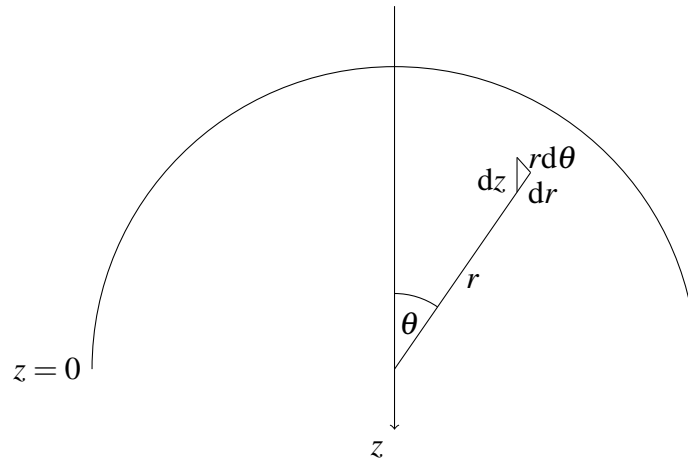


Figure 1.1: The relation between the line-of-sight depth z and polar coordinates r, θ .

By using polar coordinates centred on the star the derivative of the specific intensity with respect to geometrical depth along the line of sight (see Figure 1.1) can be written as

$$\frac{dI_v}{dz} = \frac{\partial I_v}{\partial r} \frac{dr}{dz} + \frac{\partial I_v}{\partial \theta} \frac{d\theta}{dz}$$

if we assume that I_v does not depend on the azimuthal angle ϕ . If the thickness of the atmosphere is very small compared to the radius of the star, as often is, then $\frac{d\theta}{dr} = 0$. This is known as the plane parallel approximation. The specific intensity at the stellar surface can then be written as

$$I_v(0) = \int_0^\infty \frac{S_v e^{-\frac{\tau_v}{\cos \theta}}}{\cos \theta} d\tau_v. \quad (1.10)$$

The more general spherical geometry must be used for supergiants that have extended atmospheres, but for most stars plane parallel geometry can be used. (Gray, 2005, p. 130-131)

1.1.4 Hydrostatic equilibrium

Hydrostatic equilibrium means that a star is stable because the gravity of the star is balanced by its internal pressure. The equation of hydrostatic equilibrium can be written as

$$\frac{dp}{dx} = \rho g, \quad (1.11)$$

where p is pressure, x is the depth from the stellar surface, ρ is the gas density and g is the gravitational acceleration. Hydrostatic equilibrium holds for many stars but does not apply for pulsating stars and stars with very strong stellar winds. (Gray, 2005, p. 171-173)

1.1.5 Local thermodynamic equilibrium

Stellar atmospheres can usually be assumed to be in local thermodynamic equilibrium (LTE). LTE means that the excitation of the particles of the stellar plasma is mainly determined by their mutual collisions (Gray, 2005, p. 15). If that is true, then a stellar atmosphere can be divided into thin layers with each layer having a uniquely determined temperature (Gray, 2005, p. 171). The ratio of number densities of particles in the n -th excited level N_n and all particles of the same species N in each layer is then given by the Boltzmann equation

$$\frac{N_n}{N} = \frac{g_n}{u(T)} e^{-\frac{\chi_n}{kT}}, \quad (1.12)$$

where g_n is the statistical weight, χ_n is the excitation potential of the n -th excitation level, $u(T) = \sum g_n e^{-\frac{\chi_n}{kT}}$ is the partition function, T is temperature and k is the Boltzmann constant. Additionally the ratio of number densities of $n+1$ and n times ionized particles is given by the Saha equation

$$\frac{N_{n+1}}{N_n} = \frac{2(2\pi m_e)^{\frac{3}{2}} (kT)^{\frac{5}{2}} u_{n+1}(T) e^{-\frac{I}{kT}}}{h^3 u_n(T) P_e}, \quad (1.13)$$

where m_e is the mass of an electron, I is the ionization potential of the $n+1$ -st ion, h is Planck's constant and P_e is the electron pressure. If we denote the m -th excitation level of the n -th ion as N_{nm} we obtain

$$\begin{aligned} \frac{N_{nm}}{N} &= \frac{N_{nm}}{\sum N_i}, \\ &= \frac{\frac{N_{nm}}{N_n}}{\frac{N_0}{N_n} + \dots + \frac{N_{n-1}}{N_n} + 1 + \frac{N_{n+1}}{N_n} + \dots}, \end{aligned} \quad (1.14)$$

where the ratio $\frac{N_{nm}}{N_n}$ can be found from the Boltzmann equation (1.12) and the ratios in the denominator can be computed by using the Saha equation (1.13).

The atmospheres of very hot stars cannot be assumed to be in LTE and non-LTE (NLTE) must be used (Przybilla et al., 2011). This is because of the general properties of stellar plasma. In the case of equal pressures hotter plasma has lower density than colder plasma. Lower density means less collisions between particles, so particle excitation depends more on radiation. This prevents LTE from developing i.e. the temperature that describes the speed distribution of plasma particles does not describe their excitation. (Gray, 2005, p. 15, 171)

LTE models should not be used for modelling very hot stars but the applicability of LTE models can depend on the spectral lines used for determining the stellar parameters and, in the case of very strong spectral lines, it can even depend on whether all of the line or only its wings are used. For example, Przybilla et al. (2011) showed that the LTE model ATLAS9/SYNTH (Kurucz, 1993; Kurucz and Avrett, 1981) can be used to determine the parameters of stars with effective temperatures $15000\text{K} \lesssim T_{\text{eff}} \lesssim 22000\text{K}$ if the appropriate spectral lines are used.

Different spectral lines are formed at different depths in the photosphere and consequently have different LTE breakdown temperatures. For example, the cores of strong spectral lines are formed in the upper layers of the photosphere because the absorption is very strong at the central wavelengths of the lines and photons that are emitted deeper in the atmosphere are absorbed before they escape the star. The wings of such lines are formed deeper because the absorption in the wings is not as strong as in the cores (Przybilla et al., 2011). The gas density

increases with depth, so particle excitation depends more on particle collisions and eventually LTE becomes applicable.

1.1.6 Additional factors

The presence of molecules in stellar atmospheres significantly increases the amount of computations needed for modelling stellar atmospheres because they affect the absorption coefficient of stellar plasma. However, there can be no complex molecules in hot stellar atmospheres ($T_{\text{eff}} \gtrsim 9000\text{ K}$) because the collisions between the plasma particles are energetic enough to destroy molecular bonds (Aret et al., 2008).

If an atmospheric model includes hydrodynamics then it is able to take directly into account the motion of the stellar matter and its effect on the spectrum. Most models incorporate the small and large scale motions as parametrized microturbulence and macroturbulence instead. These are additional free parameters that need to be evaluated based on observations (Gray, 2005, p. 423-424).

If different parts of the stellar disk have different radial velocities due to the rotation of the star then the radiation they emit is Doppler shifted by different amounts. The spectral lines of the stellar spectrum are therefore broadened. The faster the stellar rotation, the more spectral lines will be broadened. It is important to notice that rotational broadening is not only influenced by the speed of stellar rotation but also by the angle between the axis of stellar rotation and the line of sight. The spectral lines of even a rapidly rotating star are not rotationally broadened if the axis of rotation and the line of sight are parallel.

1.2 The formation of stellar spectra

A stellar atmosphere is composed of hot gas that is both opaque and radiating. The smaller the absorption coefficient of the gas, the deeper into the stellar atmosphere can be seen. Deeper layers of the atmosphere are also hotter and therefore they radiate more. The absorption coefficient is much higher for the central wavelengths of spectral lines than it is for the neighbouring wavelengths. The atmospheric layers that can be seen at the central wavelengths of spectral lines are therefore higher, cooler and radiate less. It can be concluded that a stellar spectrum must be an absorption spectrum, as is well known from observations.

Stellar radiation is affected by continuous and line absorption. Line absorption causes spectral lines while continuous absorption shapes the continuum. An example of a synthetic stellar

spectrum is shown on Figure 1.2. Flux is shown in the plot in spectral temperature units defined as $t_\lambda = \frac{T_\lambda}{T_{\text{eff}}}$, where T_λ is the temperature of a black body with equal flux at the wavelength λ i.e. $F_\lambda = B_\lambda(T_\lambda)$. It can be seen that the shape of the continuum is quite different from the shape of the continuum a black body would produce.

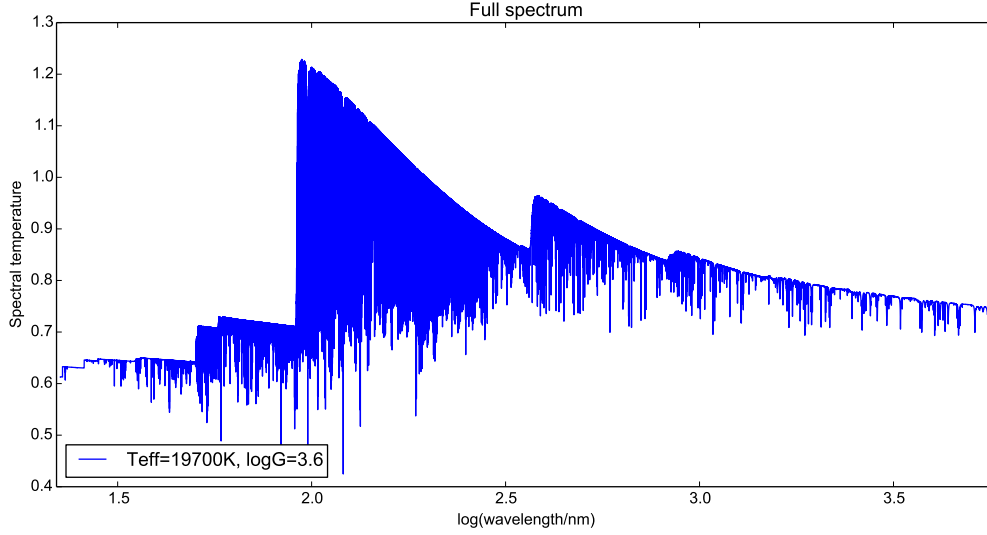


Figure 1.2: An example of a synthetic stellar spectrum. This and all other plots were made with matplotlib (Hunter, 2007).

1.2.1 Continuous absorption

Continuous absorption is caused by bound-free and free-free electron transitions. The biggest sources of continuous absorption in stars of spectral type B, which are relevant for this thesis, are the ionization and free-free transitions of neutral hydrogen (Gray, 2005, p. 154).

The effective cross section of a bound-free transition of a hydrogenic ion with mass m , charge Z and principal quantum number n is (in CGS-Gauss units (Ivanov, 1973, p. 16))

$$\kappa_{\text{bf}}(\nu) = \frac{64\pi^4 e^{10} m Z^4}{3\sqrt{3} c h^6 n^5} \frac{1}{\nu^3} g_{\text{bf}}(\nu), \quad (1.15)$$

where, e is the elementary charge, c is the speed of light and $g_{\text{bf}}(\nu)$ is a quantum mechanical correction on the order of unity known as the Gaunt factor. The free-free effective cross section per free electron is given (again in CGS-Gauss units (Ivanov, 1973, p. 18)) by

$$\kappa(\nu) = \frac{8\pi e^6 Z^2}{3\sqrt{3} m c h \sqrt{2\pi m k T}} \frac{1}{\nu^3} g_{\text{ff}}(\nu). \quad (1.16)$$

1.2.2 Line absorption

The bound-bound electron transitions produce line absorption. Spectral lines have non-zero widths due to natural broadening, pressure broadening and thermal broadening.

Natural broadening is caused by the finite lifetimes of excited states. The natural absorption coefficient per atom is given by

$$\alpha(\omega) = \frac{e^2 f \gamma}{4\epsilon_0 m c \left((\Delta\omega)^2 + \frac{\gamma^2}{4} \right)}, \quad (1.17)$$

where f is called the oscillator strength, ϵ_0 is the dielectric permeability of vacuum, γ is the damping coefficient of the spectral line and $\Delta\omega = \omega - \omega_0$ is the difference of the frequency ω and the central frequency ω_0 (Gray, 2005, p. 232-238 has details). This is a Lorentzian profile.

Pressure broadening appears due to the interaction of particles in the stellar plasma. It can be shown (Gray, 2005, p. 240-241) that for most cases the pressure broadening will also result in a Lorentzian profile. Hydrogen is a major exception as it is very strongly influenced by the linear Stark effect that is caused by the electric fields of ions around hydrogen atoms.

The random thermal motion of gas particles causes Gaussian broadening of the line given by

$$\alpha(\nu) = \frac{\sqrt{\pi} e^2 f}{m c \Delta\nu_D} e^{-\left(\frac{\Delta\nu}{\Delta\nu_D}\right)^2}, \quad (1.18)$$

where $\Delta\nu = \nu - \nu_0$ is the difference of the frequency ν from the central frequency ν_0 and $\Delta\nu_D$ is a parameter that describes the speed distribution in the gas. Microturbulence affects line absorption in the same way as thermal motion, so it can also be described by a Gaussian profile (Gray, 2005, p. 253-255).

The total line absorption coefficient is the convolution of all individual line absorption coefficients. It is the well known Voigt profile for most elements. For hydrogen the line absorption coefficient can be written as the weighted sum of a Voigt profile and the Stark profile (Gray, 2005, p. 255-259).

1.3 Atmospheric parameters

The most useful parameters for describing stellar atmospheres are temperature and pressure. The temperature of a stellar atmosphere is usually expressed by its effective temperature T_{eff}

which is defined as the temperature of a black body that emits the same amount of energy in the same amount of time and from the same surface area as the star in question. Pressure in a stellar atmosphere is determined primarily by its surface gravity as the two are related by Equation 1.11 in the case of hydrostatic equilibrium. The surface gravity is often given as $\log g$ which is the decimal logarithm of the value of the gravitational acceleration at the stellar surface in CGS units. For example, since the gravitational acceleration of Earth at its surface is $g \approx 10\text{m/s}^2 = 1000\text{cm/s}^2$, its surface gravity would be given as $\log g \approx 3$. There is usually little ambiguity in the location of a stellar surface.

T_{eff} and $\log g$ are useful and commonly used parameters that describe a stellar atmosphere as a whole, but it is important to note that both temperature and pressure in a stellar atmosphere vary with depth.

Chapter 2

Observational data

2.1 Selection criteria

The most suitable stars for the purposes of this work were single stars of spectral type B (T_{eff} between roughly 10000 K and 30000 K) and luminosity classes III to V ($\log g$ between roughly 3.0 and 4.5) with low projected rotational velocities ($v \sin i \lesssim 50 \text{ km/s}$). The spectra of multiple star systems are composed of the spectra of their components, so determining the parameters of any individual star based on the combined spectrum of the entire system can be very difficult. Too much rotational broadening can cause blending of spectral lines and also difficulties in identifying the continuum level.

2.2 Stellar sample

Lyubimkov et al. (2002) determined the surface gravities, effective temperatures and interstellar extinctions of 107 B-type stars. They also estimated the distances of the stars based on the parameter values they had obtained and found the distance estimates to be in good agreement with the parallaxes measured by the *Hipparcos* (ESA, 1997) satellite. The parameter values found by them can therefore be considered to be fairly accurate.

The stellar sample used in this work (Table 2.1) is composed of the suitable stars in the work by Lyubimkov et al. (2002) for which high-resolution archive spectra were easily obtainable.

Table 2.1: The list of analysed stars. Spectral classification by Lesh (1968) (*a*) or Houk and Smith-Moore (1988) (*b*). Projected rotational velocities by Abt et al. (2002). T_{eff} and $\log g$ by Lyubimkov et al. (2002).

HD	Spectral type	$v \sin i$ (km/s)	T_{eff} (K)	$\log g$
34816	B0.5IV ^{<i>a</i>}	25	$27\,900 \pm 400$	4.22 ± 0.11
43112	B1V ^{<i>a</i>}	0	$25\,200 \pm 900$	4.22 ± 0.15
35337	B2IV ^{<i>a</i>}	15	$22\,300 \pm 700$	4.00 ± 0.12
166182	B2IV ^{<i>a</i>}	30	$20\,000 \pm 600$	3.54 ± 0.16
34447	B2V ^{<i>b</i>}	10	$17\,900 \pm 200$	3.98 ± 0.08
186660	B3III ^{<i>a</i>}	0	$16\,700 \pm 700$	3.68 ± 0.17

2.3 Observed spectra

The observed spectra used in this work were downloaded from the ESO (European Southern Observatory) archives¹ and obtained with FEROS (Fiberfed Extended Range Optical Spectrograph, Kaufer et al. (1999)) on the ESO 2.2 m telescope in La Silla, Chile. FEROS is an echelle spectrograph with resolving power $R = 48\,000$. The spectra that were acquired were mostly reduced with only continuum normalization left undone.

2.4 Data processing

2.4.1 Radial velocities

The observed stellar spectral lines were not at their laboratory wavelengths due to the Doppler shifts caused by the movement of stars along the lines of sight. The synthetic spectra computed by SMART do not include such Doppler shifts, so they must be removed from the observed spectra. If a star moves away from us with the speed $v \ll c$, the wavelengths of radiation emitted by the star will be shifted by

$$\Delta\lambda = \frac{v}{c}\lambda_0, \quad (2.1)$$

where v is the speed of the star along the line of sight ($v > 0$ if the star moves away from us), c is the speed of light and λ_0 is the laboratory wavelength of radiation. The ratio of measured

¹Based on data products from observations made with ESO Telescopes at the La Silla Paranal Observatory under programme IDs 178.D-0361(A), 088.D-0064(A), 086.D-0714(A), 091.C-0713(A), 179.C-0197(B) and 081.C-2003(A).

and laboratory wavelengths

$$\frac{\lambda}{\lambda_0} = 1 + \frac{v}{c} \quad (2.2)$$

of narrow metal² lines were used to evaluate $1 + \frac{v}{c}$ for each star (see Table 2.2) and those values were then used to remove the Doppler shifts from the observed spectra.

Table 2.2: Measured stellar radial velocities.

HD	$1 + \frac{v}{c}$	v (km/s)
34816	0.999935	−19
43112	0.999870	−39
35337	0.999910	−27
166182	1.000050	15
34447	0.999920	−24
186660	1.000042	13

2.4.2 Normalization

The observed spectra were normalized with the Python program `specnorm.py` by Bressert et al. (2012).

2.4.3 Equivalent widths

The equivalent width of a spectral line is the width of such a unit height rectangle that has the surface area the spectral line cuts out from a normalized spectrum. The larger the equivalent width, the stronger the spectral line. A Python program was written for measuring the equivalent widths of spectral lines as

$$EW = \sum_{\lambda_{min} < \lambda < \lambda_{max}} (1 - F(\lambda)) \Delta\lambda \quad (2.3)$$

where λ_{min} and λ_{max} are the maximal and minimal wavelengths of the spectral line, $F(\lambda)$ is the relative flux at wavelength λ and $\Delta\lambda$ is the wavelength difference of adjacent data points.

²In astronomy it is customary to refer to all chemical elements except hydrogen and helium as metals. This convention is also used in this work.

Chapter 3

Computations and analysis

3.1 Program SMART

SMART is a computer program written in the programming language Fortran 90/95 for computing plane-parallel line-blanketed LTE atmospheric models and synthetic spectra of stars without convection or molecules (except H_2) in their atmospheres (see Aret et al. (2008)). Plane parallel geometry means that SMART should not be used to compute the model atmospheres of supergiants (Gray, 2005, p. 130-131). The assumptions of LTE and lack of convection and molecules limit the applicability of SMART to moderately hot stars.

The following is a brief description of the working principles of SMART which have been provided more thoroughly by Sapar (2014). The stellar atmosphere is divided into 64 layers by fixed pressure steps. First the temperature of each layer is calculated, then the excitation states of the gas particles are computed based on the Boltzmann and Saha equations ((1.12) and (1.13)). After that it is possible to compute the continuous and line absorption coefficients which in turn allow to compute the detailed flux in all layers in a given wavelength range which was chosen to be from 22.5 nm to 5760 nm in this work. The temperature distribution is corrected to achieve flux constancy by using a modified Unsöld-Lucy method (Unsöld, 1951; Lucy, 1964). The flux in the outermost layer is the synthetic spectrum produced by the model.

The working principles of SMART are illustrated in the flowchart presented in Figure 3.1.

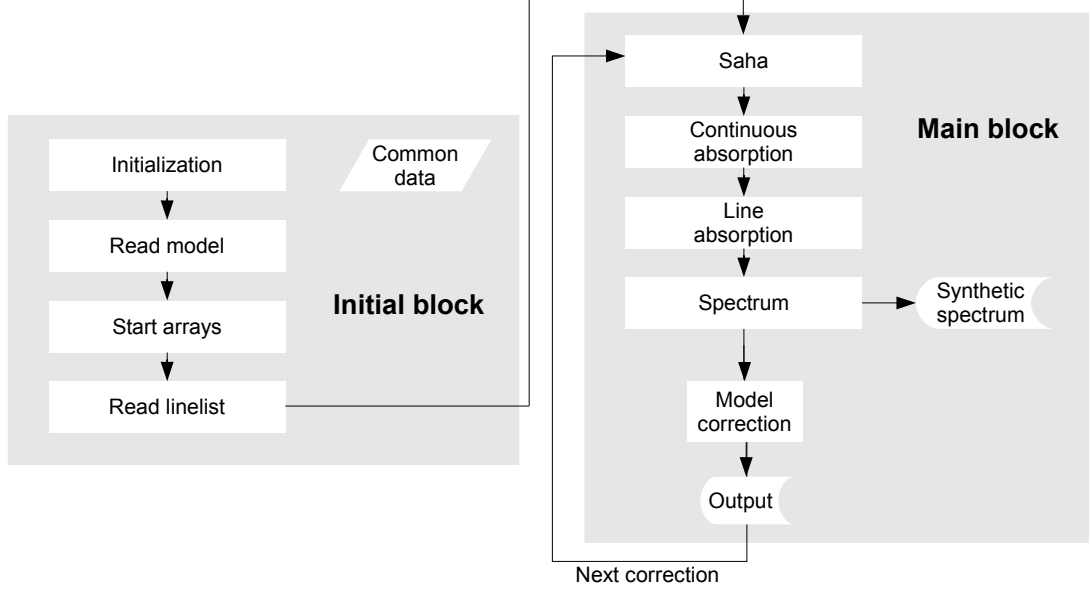


Figure 3.1: A flowchart of the working principles of SMART.

3.2 Model computations

A computer with 64 Intel® Xeon® CPU X7550 @ 2.00 GHz processors and shared physical memory approximately 1 TB was used for the model computations. Additional scripts were written to facilitate the handling of large number of both input and output files. Initially a grid of 25 models with different T_{eff} and $\log g$ values was computed for each star in the sample (see Table 2.1). T_{eff} and $\log g$ were both varied in five steps around the value provided by Lyubimkov et al. (2002), with $\log g$ rounded to the nearest tenth. The initial T_{eff} step used in the grid ranged from 200 K for the coolest star to 400 K for the hottest star. The $\log g$ step was 0.1 for all stars. All models assumed solar chemical composition and zero macroturbulence.

At first 50 iterations were computed for the cooler stars and 100 iterations for the two hotter stars in order to achieve the desired flux constancy accuracy of 0.5 %. The spectral resolution of these computations was $R = 30\,000$. Finally an additional iteration was computed for all models to obtain high-resolution synthetic spectra with spectral resolution $R = 100\,000$. Lower spectral resolution used for computing the atmospheric models was sufficient for achieving the desired flux constancy while keeping the computation times as low as possible. The size of the output files of each model (i.e. for each used T_{eff} and $\log g$ pair) was roughly 860 MB and computing 50 iterations took about 24 hours. The computed grids were used for parameter estimation and they were expanded during the parameter estimation as needed.

A typical example of flux constancy in different iterations is presented in Figure 3.2.

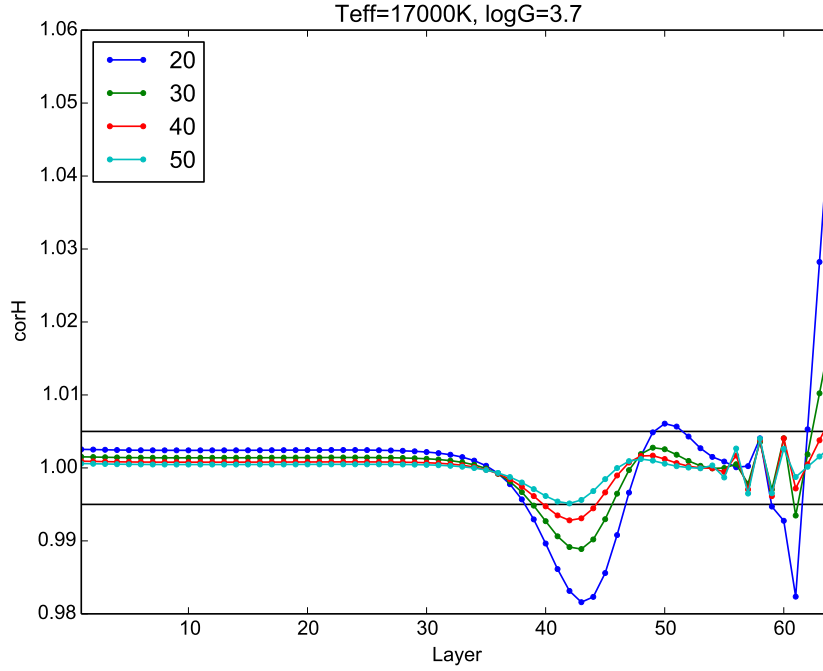


Figure 3.2: A typical example of flux constancy for different iterations (iteration number is shown in the legend). The horizontal lines mark the 0.5 % flux constancy accuracy. The first layer corresponds to the stellar surface.

3.3 Surface gravity

The wings of the Balmer lines were used as surface gravity indicators. The Balmer lines are spectral lines of neutral hydrogen produced by electron transitions where the lower level involved is the first excited level (principal quantum number $n = 2$). The Balmer lines are affected by both T_{eff} and $\log g$, but the influence of T_{eff} is relatively weak, as illustrated by Figures 3.3 and 3.4, and they are often used to evaluate the surface gravities of B-type stars (see for example Kilian et al. (1991), Hunter et al. (2007) or Lyubimkov et al. (2002)). According to Przybilla et al. (2011) the cores of Balmer lines are strongly affected by NLTE effects, but the wings that form much deeper in the stellar atmosphere are not. It is therefore possible to obtain the stellar surface gravity estimates of quite hot stars by comparing the wings of the observed Balmer lines with the synthetic spectra even if a pure LTE model is used.

Table 3.1: The wavelengths of the relevant Balmer lines.

Line	Wavelength (nm)
H β	486.1
H γ	434.1
H δ	410.2

Initial surface gravity estimations were done using the effective temperatures provided by Lyubimkov et al. (2002). Surface gravity estimation was performed again for all the new effective temperature values obtained during parameter estimation until the results converged.

The cores of the Balmer lines were of no interest due to the limitations of the used pure LTE model and systematic differences between the cores of the observed Balmer lines and the synthetic spectra are to be expected.

The comparison of different synthetic spectra with the observed spectra allows to estimate the uncertainty of the obtained surface gravity values.

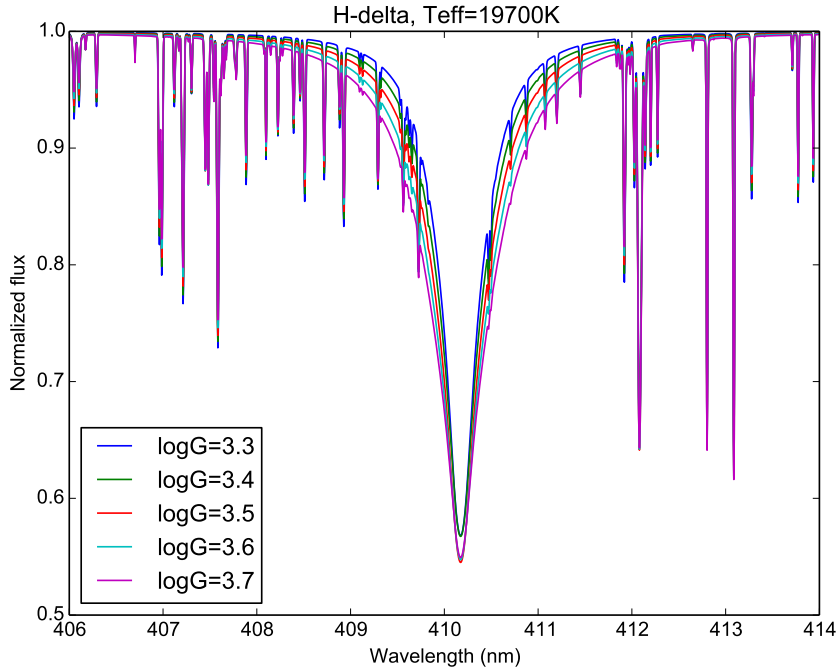


Figure 3.3: The Balmer lines are strongly influenced by surface gravity as can be seen from the synthetic spectra.

3.4 Effective temperature

The effective temperatures of B-type stars are often evaluated from the ratios of the equivalent widths of the spectral lines of adjacent silicon ionization stages (see again Kilian et al. (1991) and Hunter et al. (2007)). However, according to Przybilla et al. (2011) silicon lines are quite strongly affected by NLTE effects while oxygen lines are not. It was therefore decided to use oxygen lines for estimating the effective temperatures instead. The use of equivalent width ratios rather than the equivalent ratios themselves means that the exact stellar chemical composition is not very important. This makes the solar chemical composition used in our modelling a good approximation.

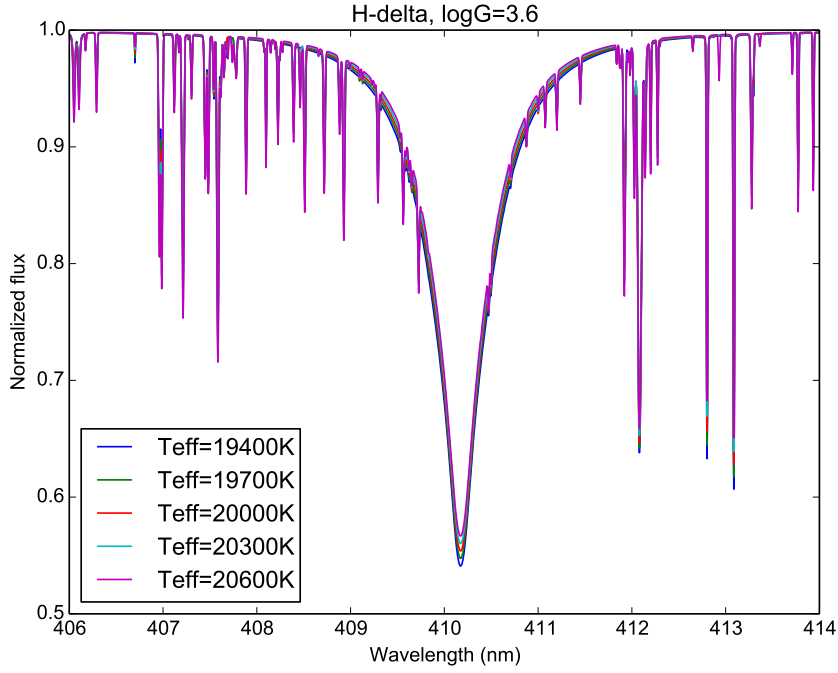


Figure 3.4: The Balmer lines are weakly influenced by effective temperature as can be seen from the synthetic spectra.

The O I¹ lines and the first group of O II lines (see Table 3.2) were used for HD 166182 and cooler stars, but there were no identifiable O I lines in the spectra of hotter stars. It was decided to use the comparison of the first group of O II lines with the second group of O II lines for HD 166182 and hotter stars. The Python program described in Subsection 2.4.3 was used to find the equivalent widths of the relevant spectral lines in all of the available synthetic spectra with the log g value found from the Balmer wings. Because the O I lines were somewhat blended, the total equivalent width of those lines was used instead of individual equivalent widths. Least squares quadratic polynomial fitting was used to estimate the ratio of equivalent widths as a function of effective temperature for a given surface gravity value and the measured equivalent width ratio of the observed spectra was then used to find the T_{eff} values. An example of fitting is presented in Figure 3.5. A Python program was written that performed all these steps automatically. Temperature estimation was performed again whenever

Table 3.2: The spectral lines used for determining effective temperatures. Laboratory wavelengths from Kramida et al. (2014).

Group	Wavelength (nm)
O I	615.598
	615.677
	615.818
1st group of O II	441.491
	441.697
2nd group of O II	494.107
	495.571

¹O I means neutral oxygen, O II means once-ionized oxygen etc.

the surface gravity values changed during parameter estimation until the results converged.

Evaluating the effective temperatures from the equivalent width ratios of several different line pairs allows to estimate the effective temperature uncertainties.

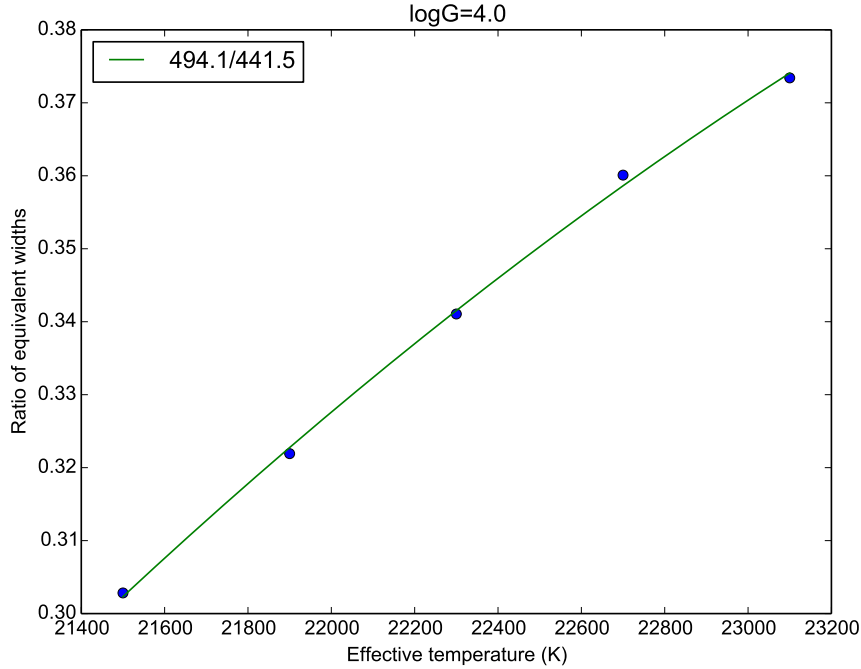


Figure 3.5: An example of a quadratic polynomial that describes the equivalent width ratio as a function of temperature. This example depicts the equivalent width ratios of the O II $\lambda\lambda$ 4941 and 4415 lines.

3.5 Spectral broadening

The observed spectral lines were broadened due to stellar rotation and the limited resolution of the spectrograph. In order to visually compare the observed and synthetic spectra, the synthetic spectra must be convolved with what are called the rotational profile (Gray, 2005, p. 458-467) and the instrumental profile (Gray, 2005, p. 274-277). These convolutions make the spectral lines wider but do not change their equivalent widths. We used the auxiliary files to the program SPECTRUM by Gray (2010) to achieve this. The projected rotational velocities were taken from Abt et al. (2002). The instrumental profile was approximated by a simple Gaussian profile.

Rotational and instrumental broadening does not significantly influence the Balmer lines as they are very wide compared to the instrumental and rotational profiles. Applying this broadening would also make the equivalent width measurements of the oxygen lines less reliable due to line blending. Rotational and instrumental broadening was therefore only applied to the final synthetic spectra after parameter estimation was completed.

Chapter 4

Results and discussion

The values of T_{eff} and $\log g$ of the sample stars determined in this work and by Lyubimkov et al. (2002) can be seen in Table 4.1 along with the estimated parameter uncertainties. The relevant spectral regions of the observed and best-fit synthetic spectra can be found in appendix A. The main sources of uncertainty are the effects caused by macroturbulence, the differences of the stellar chemical compositions from the solar chemical composition used in modelling, the noise present in the observed spectra, the uncertainties in continuum estimation (which is connected to the presence of spectral noise) and the simplifications involved in SMART itself. It must also be noted that uncertainty in surface gravity increases the uncertainty of effective temperature and vice versa, as the Balmer lines that were used to estimate the surface gravity are also somewhat influenced by temperature and oxygen ionization that was used to estimate the temperature is somewhat affected by surface gravity.

Table 4.1: The stellar parameters determined in this work (left) and by Lyubimkov et al. (2002) (right).

HD	T_{eff} (K)	$\log g$	T_{eff} (K)	$\log g$
34816	20350 ± 1250	4.0 ± 0.2	27900 ± 400	4.22 ± 0.11
43112	22900 ± 300	4.0 ± 0.2	25200 ± 900	4.22 ± 0.15
35337	21500 ± 500	4.0 ± 0.1	22300 ± 700	4.00 ± 0.12
166182	19700 ± 800	3.6 ± 0.1	20000 ± 600	3.54 ± 0.16
34447	17200 ± 150	3.8 ± 0.1	17900 ± 200	3.98 ± 0.08
186660	16300 ± 200	3.6 ± 0.1	16700 ± 700	3.68 ± 0.17

The parameter estimates are quite similar for most of the stars in our sample but for the two hotter stars the results do not agree (the difference of T_{eff} values of HD 34447 can be considered to be quite small). The minimal temperature at which the methods used in this work fail to give good results seems to lie somewhere between 22 000 K and 25 000 K. This agrees well with the

work by Przybilla et al. (2011) who studied the applicability of the LTE model ATLAS9/SYNTH (Kurucz, 1993; Kurucz and Avrett, 1981) and found the highest temperature for which pure LTE modelling still gave good results to be roughly 22000 K. This seems to imply that the disagreement between the results obtained with SMART and the results by Lyubimkov et al. (2002) for the two hotter stars are not due to programming errors in SMART, inaccurate atomic data or faulty implementation of parameter estimation methods, but rather because of the inapplicability of LTE for stars that hot. There is no indication that SMART cannot be used to evaluate the parameters of stars with effective temperatures between roughly 16000 K and 22000 K by using the methodology described in and implemented as a part of this work. The good agreement for the cooler stars is especially remarkable as Lyubimkov et al. (2002) used not only a different model atmosphere program (ATLAS, Kurucz (1993)), but also a different method for estimating the effective temperatures. In their work synthetic colour indices were used instead of spectral line equivalent width ratios.

The O II $\lambda 4417$ line is blended with a Fe II line in the spectra of stars cooler than $T_{\text{eff}} \sim 20000$ K. This proved not to be a problem and the temperature estimates obtained by using this oxygen line were consistent with the results obtained with the O II $\lambda 4415$ line that was not blended. NLTE effects were apparently negligible for iron as well as for oxygen in the cooler cases where blending was significant.

The goal of writing software that would allow the estimation of stellar parameters was successfully achieved. Temperature was estimated from the equivalent width ratios of oxygen lines but modifying the software to use some other element instead requires only minimal effort.

The stellar sample used in this work covered the desired temperature range quite well and included all the stars from the work by Lyubimkov et al. (2002) that fitted the criteria discussed in Section 2.1 and for which high-resolution spectra obtained with FEROS (Kaufer et al., 1999) were available. However, the sample size was still rather small so the results of this work can only be considered to be preliminary and should be used with reasonable caution. The implications of this work can be made more reliable by increasing the stellar sample, especially by including stars with $T_{\text{eff}} < 16000$ K. Further work for testing the applicability of SMART can also include the implementation and validation of methods of estimating chemical abundances of different chemical elements and macroturbulence.

Validation of SMART stellar atmosphere models

Eero Vaher

Summary

SMART is a computer program written at the Tartu Observatory that enables to compute the atmospheric models and synthetic spectra of moderately hot stars (Aret et al., 2008). SMART has been especially useful for modelling chemically peculiar stars due to the implementation of light-induced drift (Sapar et al., 2009). However, the range of validity of SMART had not been tested yet.

The purpose of this thesis was to test the range of applicability and precision of SMART by estimating the effective temperatures and surface gravities of moderately hot stars by comparing the observed spectra with synthetic spectra computed by SMART. Extensive stellar atmospheric model computations were carried out and software suitable for stellar parameter estimation was developed.

The hydrogen Balmer lines were used to estimate the surface gravities and the equivalent width ratios of different oxygen spectral lines were used to estimate the effective temperatures. A Python program was written to accomplish this. The observed high-resolution stellar spectra were obtained from the European Southern Observatory archives. The effective temperatures and surface gravities of the stars modelled by us were compared with the values obtained by Lyubimkov et al. (2002).

The stellar parameters found by us and by Lyubimkov et al. (2002) were in good agreement for stars with $T_{\text{eff}} \lesssim 22\,000\text{ K}$, but were significantly different for hotter stars. The work by Przybilla et al. (2011) suggests that the reason for this is the inapplicability of local thermodynamic equilibrium assumed in SMART for the case of the hotter stars.

Our results suggest that SMART can be used to reliably compute the atmospheric models and synthetic spectra of stars with T_{eff} between roughly 16 000 K and 22 000 K. SMART seems to be unable to accurately model the spectra of stars hotter than $T_{\text{eff}} \approx 25\,000\text{ K}$ due to the limitations of the local thermodynamic equilibrium assumption. The lower temperature limit is yet to be determined because the results for the coolest star in our sample with $T_{\text{eff}} \approx 16\,000\text{ K}$ were accurate.

Täheatmosfäärimodelite SMART valideerimine

Eero Vaher

Kokkuvõte

SMART on Tartu Observatooriumis kirjutatud arvutiprogramm mõõdukalt kuumade tähtede atmosfäärimodelite ja sünteetiliste spektrite arvutamiseks (Aret et al., 2008). Programmi SMART abil on arvutatud valgusindutseeritud triivi keemiliselt iseäralike tähtede modelleerimisel (Sapar et al., 2009). Selle rakendatavuse piiranguid polnud aga seni testitud.

Käesoleva bakalaureusetöö eesmärgiks oli testida programmi SMART rakendatavuse piire kasutades seda tähtede efektiivsete temperatuuride ning pinnagravitatsioonide määramiseks sünteetiliste ning vaadeldud tähespektrite võrdlemise teel. Selleks sai läbi viidud mahukad mudelatmosfääride arvutused ning kirjutatud täheparameetrite määramiseks vajalik tarkvara.

Raskuskiirenduse määramiseks kasutati vesiniku Balmeri seeria jooni ning efektiivse temperatuuri hinnang saadi erinevate hapniku spektrijoonte ekvivalentlaiduste suhete mõõtmisest. Suure lahutusega vaadeldud spektrid saadi Euroopa Lõunaobservatooriumi arhiividest. Meie temperatuuri ja raskuskiirenduse hinnanguid võrreldi Lyubimkov et al. (2002) töös määratud väärtustega.

Meie töös ning Lyubimkov et al. (2002) leitud täheparameetrite väärtused olid omavahel heas kooskõlas nende tähtede jaoks, mille $T_{\text{eff}} \lesssim 22\,000\text{ K}$, kuid erinesid oluliselt kuumemate tähtede korral. Przybilla et al. (2011) tööst järeldeb, et selle põhjuseks on SMARTis kasutatud lokaalse termodünaamilise tasakaalu eelduse kohaldamatus kuumemate tähtede modelleerimisel.

Meie tulemused viitavad, et SMART võimaldab edukalt arvutada täheatmosfääride mudeleid ja sünteetilisi spektreid selliste tähtede jaoks, mille T_{eff} on vahemikus umbes $16\,000\text{ K}$ kuni $22\,000\text{ K}$. SMART ei paista olevat suuteline välja arvutama kuumemate kui $T_{\text{eff}} \approx 25\,000\text{ K}$ tähtede spektreid lokaalse termodünaamilise tasakaalu eelduse piirangute tõttu. Temperatuuri alampiiri määrata ei õnnestunud, kuna valimi kõige jahedama tähe ($T_{\text{eff}} \approx 16\,000\text{ K}$) spektri modelleerimine õnnestus hästi.

Acknowledgements

I use this opportunity to thank my supervisors Anna Aret and Boris Deshev for the feedback they provided during my work and especially for helping me get started with Linux. I am also grateful to Taavi Tuvikene for showing me how to work with observed spectra without having to quit using Python and to Arved Sapar for introducing me to stellar atmosphere modelling.

I also wish to thank the Tartu Observatory for allowing me to use their computer resources without which it might not have been possible to perform the computations that were necessary for my thesis.

Bibliography

- Abt, H. A., Levato, H., and Grosso, M. (2002). Rotational Velocities of B Stars. *The Astrophysical Journal*, 573:359–365.
- Aret, A., Sapar, A., Poolamäe, R., and Sapar, L. (2008). SMART a computer program for modelling stellar atmospheres. In Deng, L. and Chan, K. L., editors, *IAU Symposium*, volume 252 of *IAU Symposium*, pages 41–42.
- Bressert, E., Creighton, N., and Degroote, P. (2012). `specnorm.py`. An interactive spectrum normalizer, [Online]. Available: <http://python4esac.github.io/plotting/specnorm.html>.
- ESA (1997). The Hipparcos and Tycho Catalogues. ESA SP-1200.
- Gray, D. F. (2005). *The Observation and Analysis of Stellar Photospheres*. Cambridge University Press, 3rd edition.
- Gray, R. O. (2010). SPECTRUM (ver. 2.76). [Online]. Available: <http://www.appstate.edu/~grayro/spectrum/spectrum.html> Department of Physics and Astronomy, Appalachian State University.
- Houk, N. and Smith-Moore, M. (1988). *Michigan Catalogue of Two-dimensional Spectral Types for the HD Stars. Volume 4, Declinations -26°.0 to -12°.0*.
- Hunter, I., Dufton, P. L., Smartt, S. J., Ryans, R. S. I., Evans, C. J., Lennon, D. J., Trundle, C., Hubeny, I., and Lanz, T. (2007). The VLT-FLAMES survey of massive stars: surface chemical compositions of B-type stars in the Magellanic Clouds. *Astronomy and Astrophysics*, 466:277–300.
- Hunter, J. D. (2007). Matplotlib: A 2D graphics environment. *Computing In Science & Engineering*, 9(3):90–95.

- Ivanov, V. V. (1973). *Transfer of radiation in spectral lines*. NBS Special Publication, Washington: US Department of Commerce, National Bureau of Standards.
- Kaufer, A., Stahl, O., Tubbesing, S., Nørregaard, P., Avila, G., Francois, P., Pasquini, L., and Pizzella, A. (1999). Commissioning FEROS, the new high-resolution spectrograph at La-Silla. *The Messenger*, 95:8–12. FEROS.
- Kilian, J., Becker, S. R., Gehren, T., and Nissen, P. E. (1991). Chemical abundances in early B-type stars. III - NLTE temperature and gravity determination. *Astronomy and Astrophysics*, 244:419–424.
- Kramida, A., Ralchenko, Y., Reader, J., and NIST ASD Team (2014). NIST Atomic Spectra Database (ver. 5.2), [Online]. Available: <http://physics.nist.gov/asd> National Institute of Standards and Technology, Gaithersburg, MD.
- Kurucz, R. L. (1993). CD-ROM no. 13. Cambridge, Mass.: SAO.
- Kurucz, R. L. and Avrett, E. H. (1981). Solar Spectrum Synthesis. I. A Sample Atlas from 224 to 300 nm. *SAO Special Report*, 391.
- Lesh, J. R. (1968). The Kinematics of the Gould Belt: an Expanding Group? *The Astrophysical Journal Supplement*, 17:371.
- Lucy, L. B. (1964). A Temperature-Correction Procedure. *SAO Special Report*, 167:93.
- Lyubimkov, L. S., Rachkovskaya, T. M., Rostopchin, S. I., and Lambert, D. L. (2002). Surface abundances of light elements for a large sample of early B-type stars - II. Basic parameters of 107 stars. *Monthly Notices of the Royal Astronomical Society*, 333:9–26.
- Przybilla, N., Nieva, M.-F., and Butler, K. (2011). Testing common classical LTE and NLTE model atmosphere and line-formation codes for quantitative spectroscopy of early-type stars. *Journal of Physics Conference Series*, 328(1):012015.
- Sapar, A. (2014). Tarkvarast SMART tähe mudelatmosfääride ja spektrite arvutamiseks. *Tartu Tähetorni kalender*.
- Sapar, A., Aret, A., Sapar, L., and Poolamäe, R. (2009). Modelling of mercury isotope separation in CP stellar atmospheres: Results and problems. *New Astronomy Reviews*, 53:240–245.
- Unsöld, A. (1951). Ein rasch konvergierendes Iterationsverfahren zur Lösung von Strahlungsgleichgewichts-Problemen. *Naturwissenschaften*, 38:525–526.

Appendix A

Comparison of synthetic and observed spectra

The following figures depict the spectral regions of observed and best-fit rotationally and instrumentally broadened synthetic spectra that were of interest in this work.

Disagreements between the observed and synthetic spectra in the cores of the Balmer lines are due to NLTE effects. Differences in the strengths of the metal lines are due to a combination of the stellar chemical compositions being different from the solar chemical composition used in modelling, NLTE effects and also inaccurate atomic data used in modelling.

The wavelengths of the spectral lines used for determining the stellar parameters are listed here as a reminder.

Table A.1: The spectral lines used for determining stellar parameters. Laboratory wavelengths of oxygen lines from Kramida et al. (2014).

Spectral lines	Wavelength (nm)
H β	486.1
H γ	434.1
H δ	410.2
O I	615.598
	615.677
	615.818
1st group of O II	441.491
	441.697
2nd group of O II	494.107
	495.571

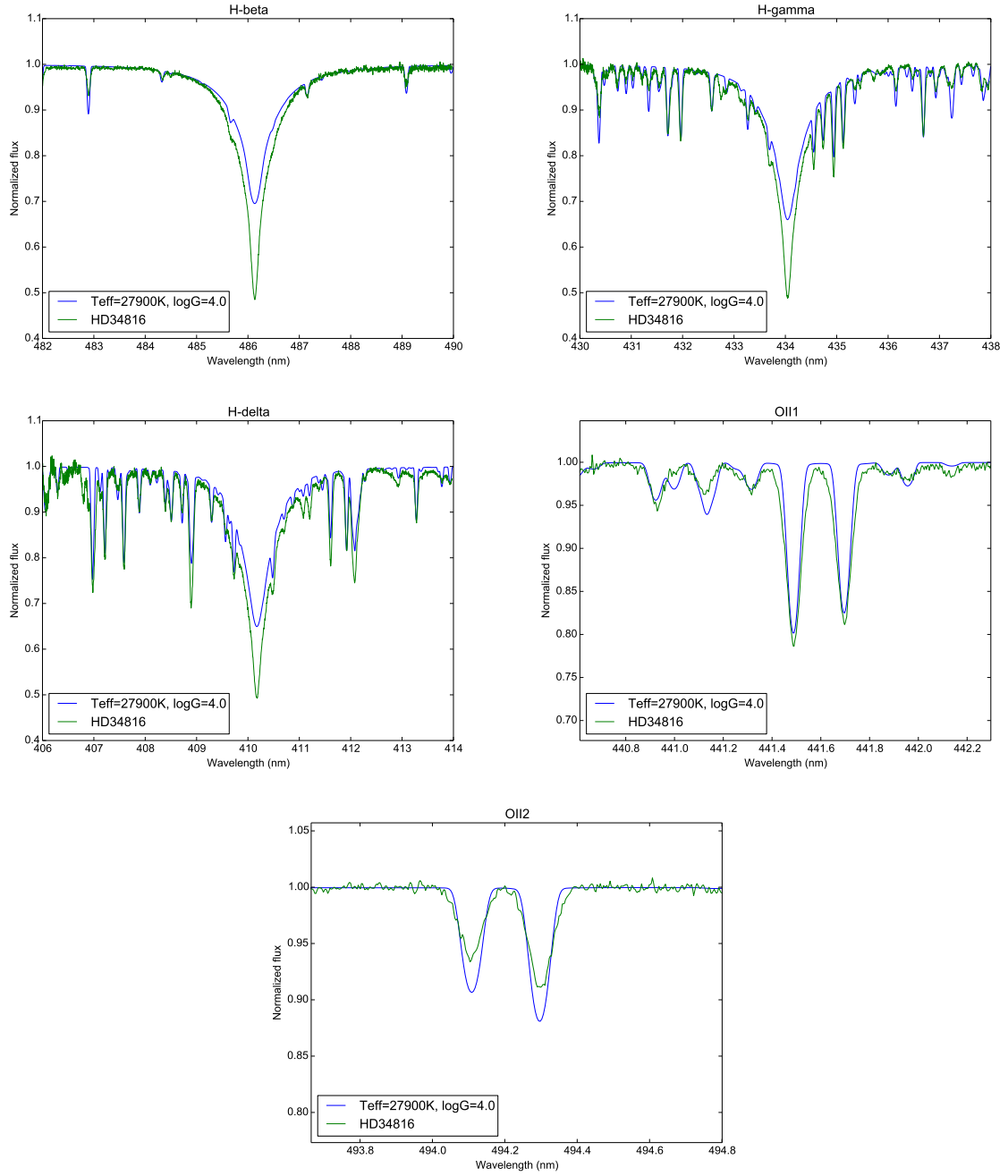


Figure A.1: The comparison of the observed and best-fit synthetic spectra of HD34816.

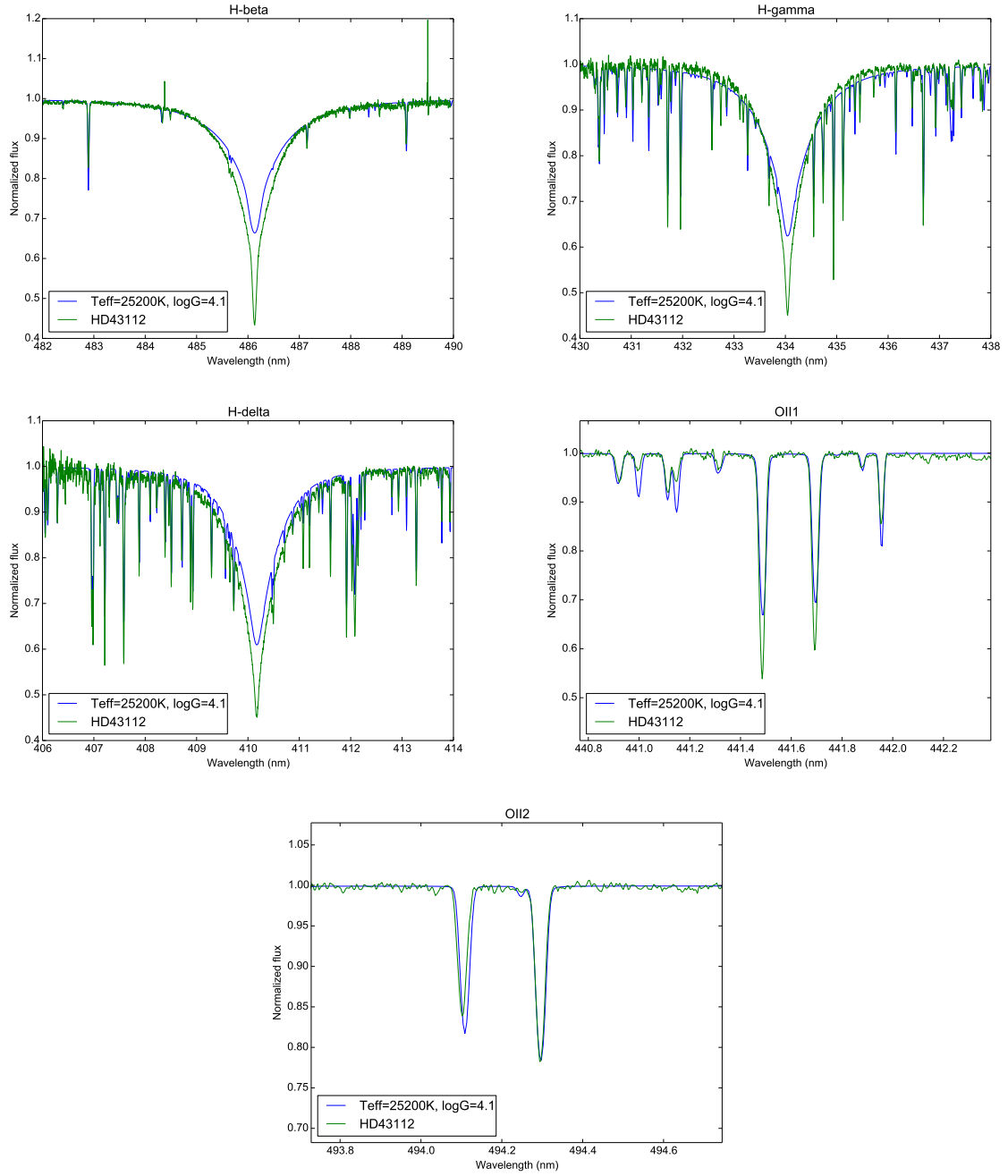


Figure A.2: The comparison of the observed and best-fit synthetic spectra of HD43112.

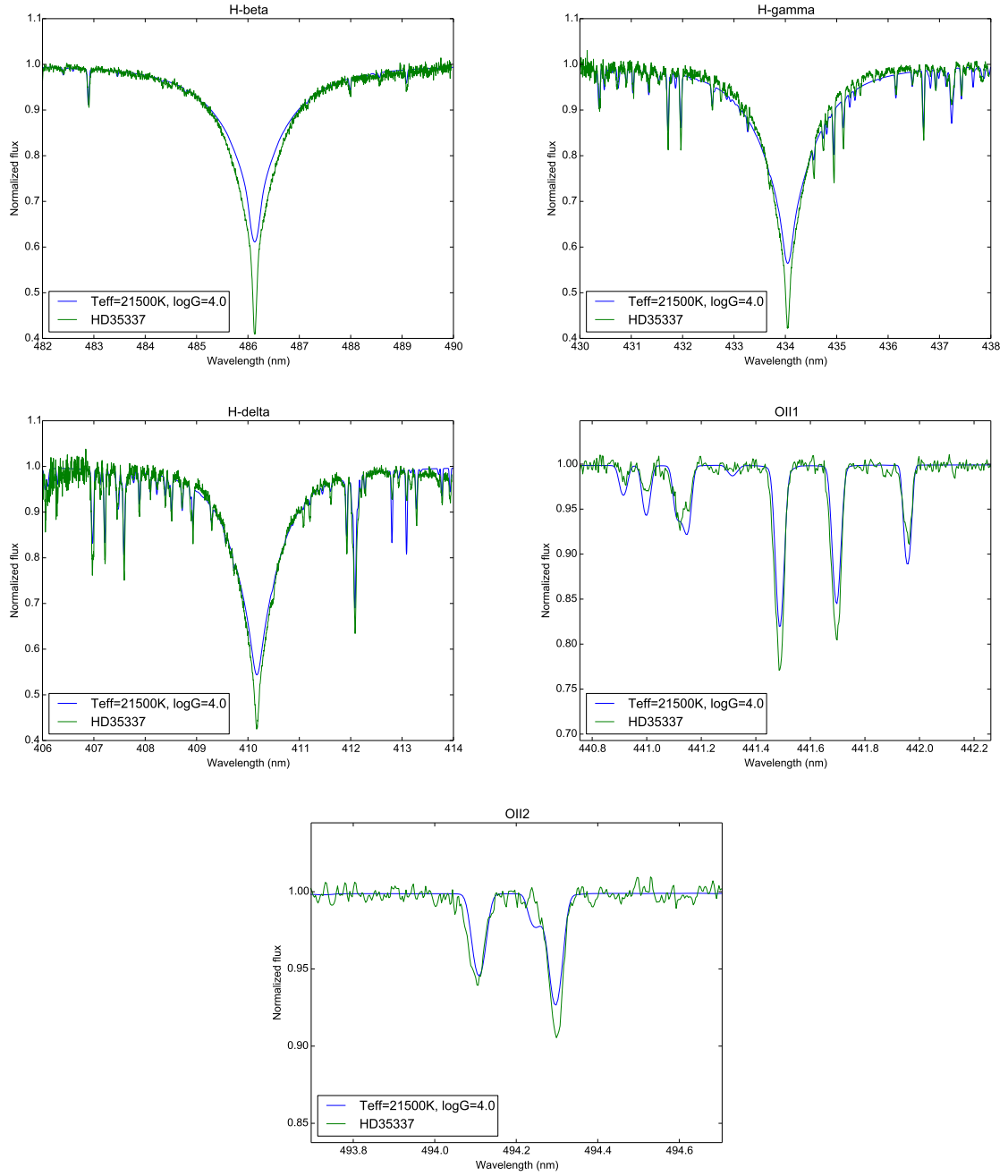


Figure A.3: The comparison of the observed and best-fit synthetic spectra of HD35337.

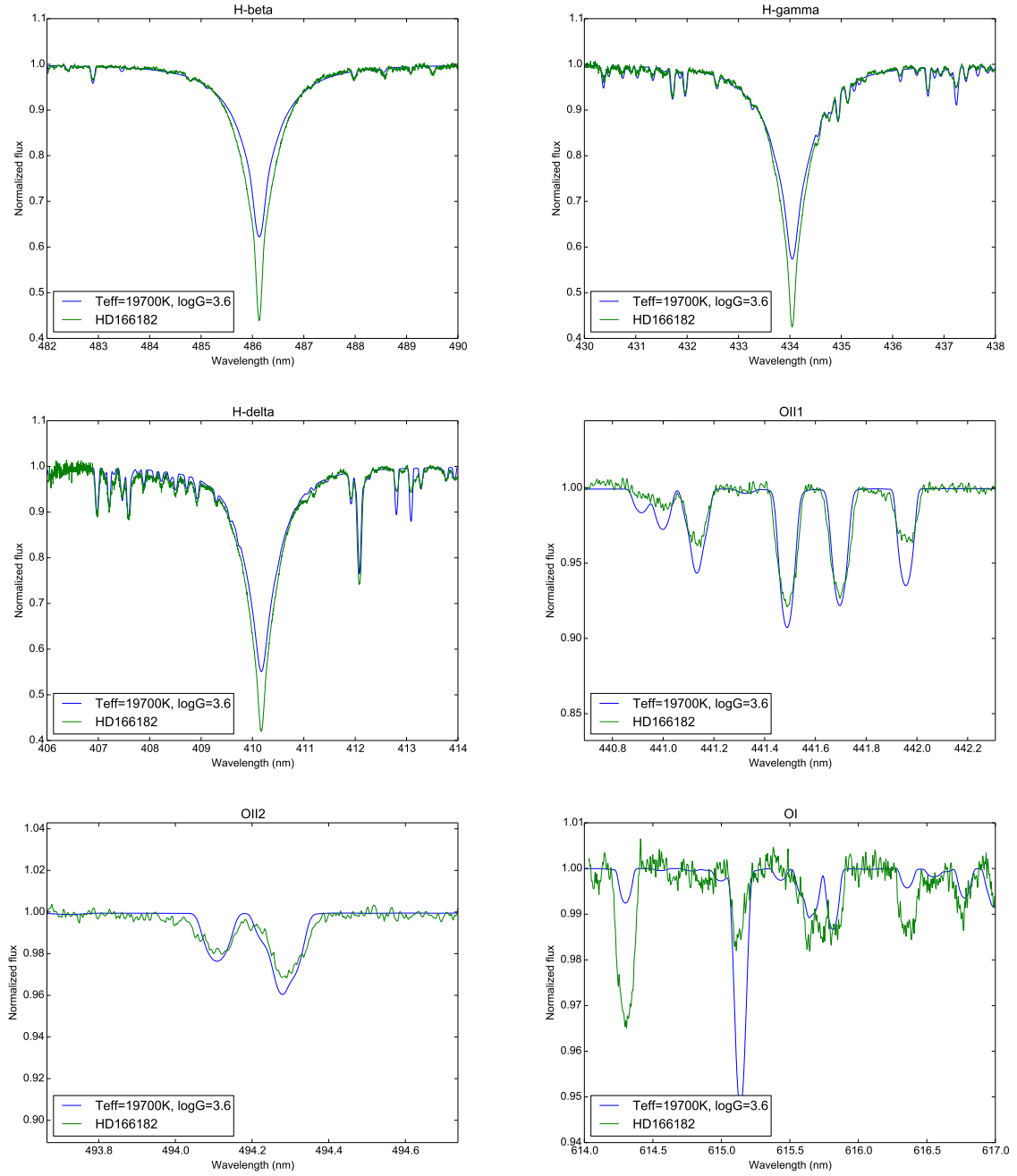


Figure A.4: The comparison of the observed and best-fit synthetic spectra of HD166182.

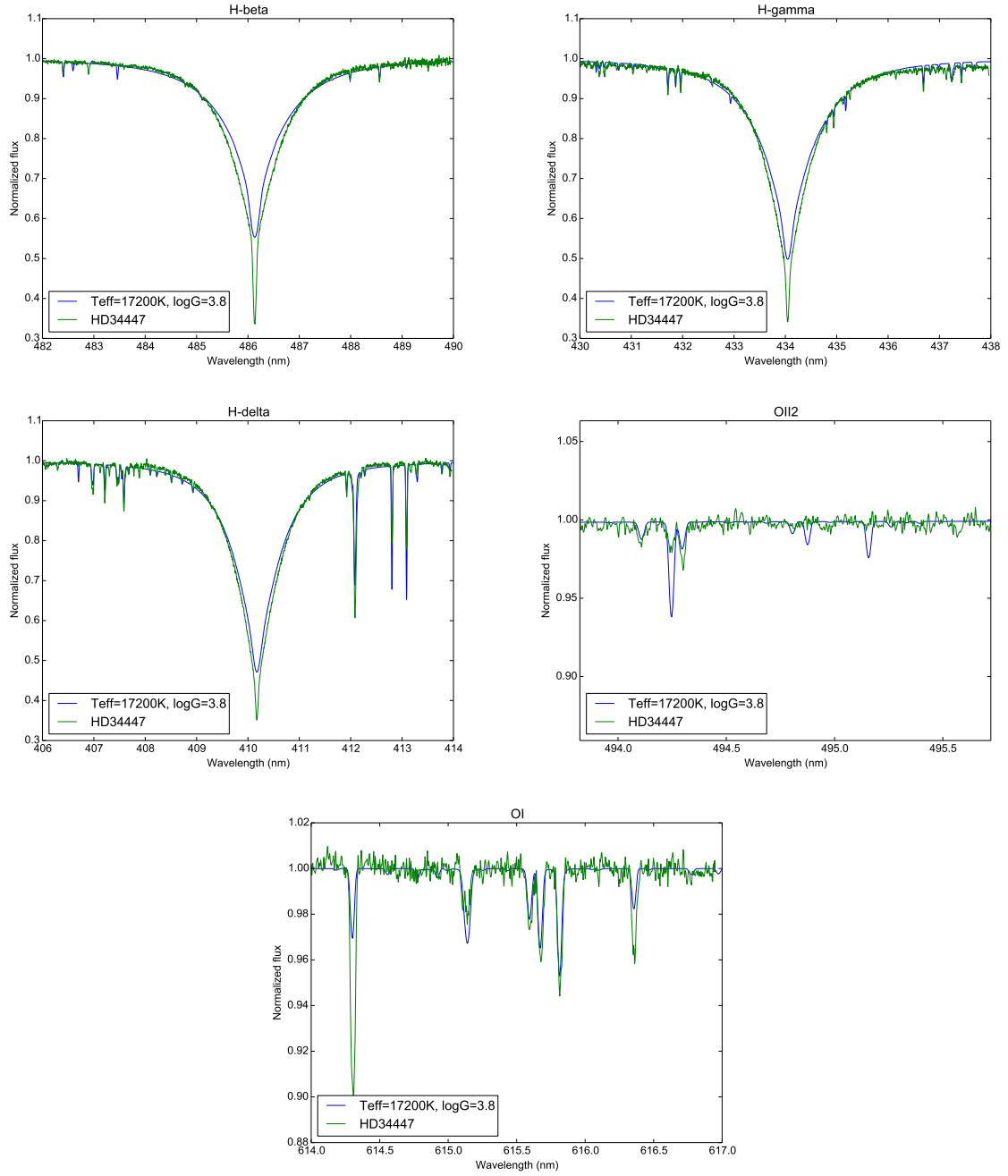


Figure A.5: The comparison of the observed and best-fit synthetic spectra of HD34447.

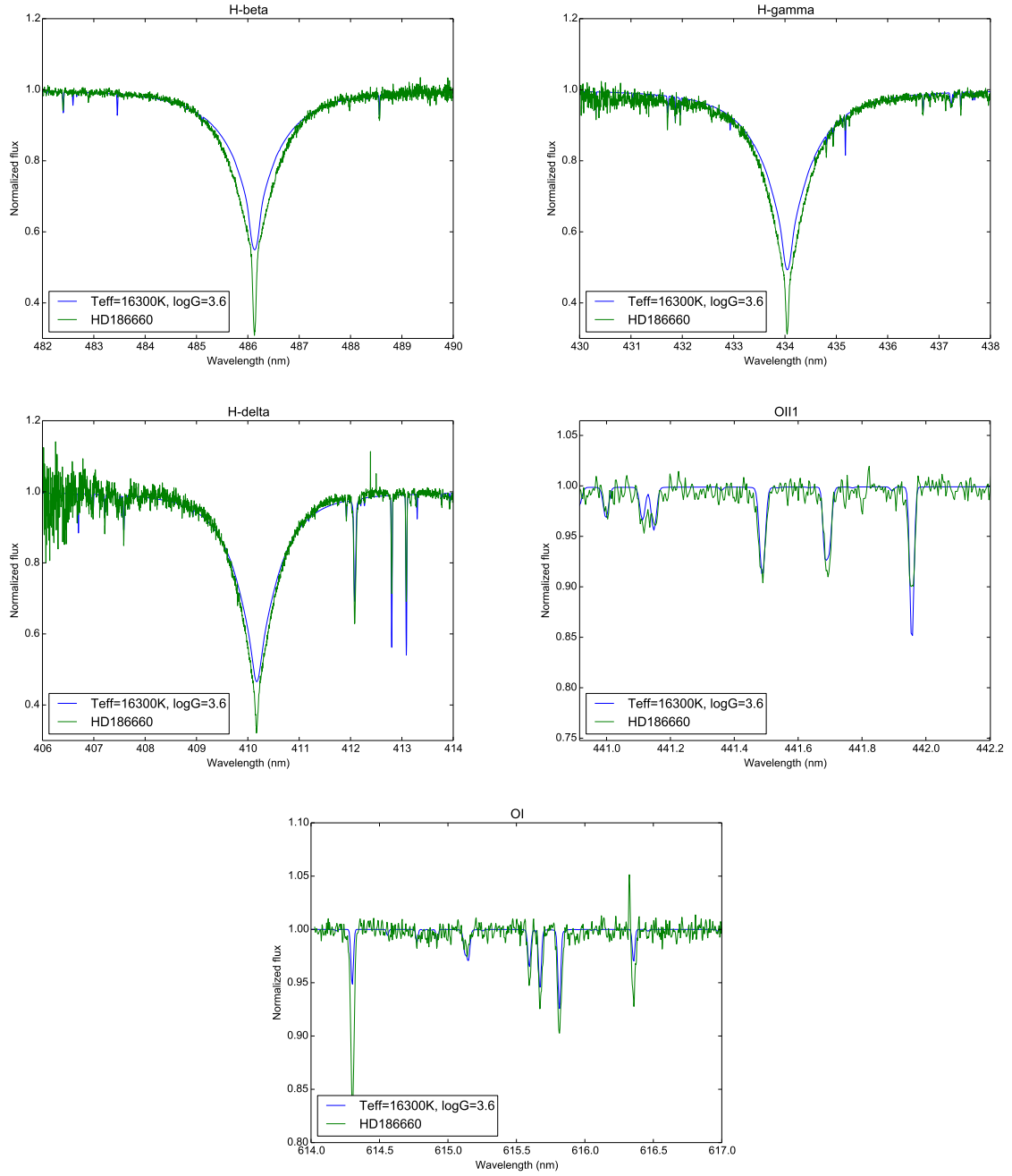


Figure A.6: The comparison of the observed and best-fit synthetic spectra of HD186660.

Lihtlitsents lõputöö reprodutseerimiseks ja lõputöö üldsusele kättesaadavaks tegemiseks

Mina, Eero Vaher,

1. annan Tartu Ülikoolile tasuta loa (lihtlitsentsi) enda loodud teose

”Validation of SMART stellar atmosphere models”,

mille juhendajad on Anna Aret ja Boris Deshev,

- (a) reprodutseerimiseks säilitamise ja üldsusele kättesaadavaks tegemise eesmärgil, sealhulgas digitaalarhiivi DSpace-is lisamise eesmärgil kuni autoriõiguse kehtivuse tähtaja lõppemiseni;
 - (b) üldsusele kättesaadavaks tegemiseks Tartu Ülikooli veebikeskkonna kaudu, sealhulgas digitaalarhiivi DSpace'i kaudu kuni autoriõiguse kehtivuse tähtaja lõppemiseni.
2. olen teadlik, et punktis 1 nimetatud õigused jäävad alles ka autorile.
 3. kinnitan, et lihtlitsentsi andmisega ei rikuta teiste isikute intellektuaalomandi ega isikuandmete kaitse seadusest tulenevaid õigusi.

Tartus, **25.05.2015**